© American Society for Mass Spectrometry, 2015

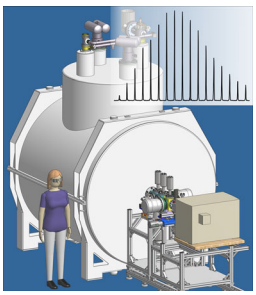
J. Am. Soc. Mass Spectrom. (2015)
DOI: 10.1007/s13361-015-1182-2

RESEARCH ARTICLE

21 Tesla Fourier Transform Ion Cyclotron Resonance Mass Spectrometer: A National Resource for Ultrahigh Resolution Mass Analysis

Christopher L. Hendrickson,[1,2] John P. Quinn,[1] Nathan K. Kaiser,[1] Donald F. Smith,[1] Greg T. Blakney,[1] Tong Chen,[2] Alan G. Marshall,[1,2] Chad R. Weisbrod,[1] Steven C. Beu[3]

[1]National High Magnetic Field Laboratory, Florida State University, 1800 East Paul Dirac Drive, Tallahassee, FL 32310, USA
[2]Department of Chemistry and Biochemistry, Florida State University, 95 Chieftain Way, Tallahassee, FL 32306, USA
[3]S. C. Beu Consulting, 12449 Los Indios Trail, Austin, TX 78729, USA



Abstract. We describe the design and initial performance of the first 21 tesla Fourier transform ion cyclotron resonance (FT-ICR) mass spectrometer. The 21 tesla magnet is the highest field superconducting magnet ever used for FT-ICR and features high spatial homogeneity, high temporal stability, and negligible liquid helium consumption. The instrument includes a commercial dual linear quadrupole trap front end that features high sensitivity, precise control of trapped ion number, and collisional and electron transfer dissociation. A third linear quadrupole trap offers high ion capacity and ejection efficiency, and rf quadrupole ion injection optics deliver ions to a novel dynamically harmonized ICR cell. Mass resolving power of 150,000 ($m/\Delta m_{50\%}$) is achieved for bovine serum albumin (66 kDa) for a 0.38 s detection period, and greater than 2,000,000 resolving power is achieved for a 12 s detection period. Externally calibrated broadband mass measurement accuracy is typically less than 150 ppb rms, with resolving power greater than 300,000 at m/z 400 for a 0.76 s detection period. Combined analysis of electron transfer and collisional dissociation spectra results in 68% sequence coverage for carbonic anhydrase. The instrument is part of the NSF High-Field FT-ICR User Facility and is available free of charge to qualified users.

Keywords: FT-ICR, FTMS, Fourier transform mass spectrometry

Received: 5 March 2015/Revised: 28 April 2015/Accepted: 30 April 2015

Introduction

High field Fourier transform ion cyclotron resonance (FT-ICR) mass spectrometry offers the highest achievable broadband mass resolving power and mass accuracy of any mass analyzer [1, 2]. Resolving power and spectral acquisition rate improve linearly, and mass accuracy and dynamic range improve quadratically with magnetic field [3]. Resolving power greater than 1 million and mass accuracy better than 1 ppm become routine at sufficiently high magnetic field strength, and high resolving power and mass accuracy can be combined with on-line LC separation and MS/MS [4]. Consequently, increased magnetic field has been a persistent goal in FT-ICR instrument development. However, the expense and complexity of superconducting magnets scale with a high power of the field strength, so fewer labs are able to acquire and support the highest field systems. We report here the design, construction, and characterization of the first 21 tesla FT-ICR mass spectrometer, which is the highest field system to date. The instrument is part of the National High Field FT-ICR User Facility at the National High Magnetic Field Laboratory (NHMFL), and is available to all qualified users.

Experimental

Reagents and Sample Preparation

Bovine serum albumin (BSA) and carbonic anhydrase (CA) were used as received from Sigma-Aldrich (St. Louis, MO, USA) and diluted to 1 μM in 49:49:1 methanol:water:formic acid. Seven standard peptides (Sigma-Aldrich) were diluted in 49:49:1 acetonitrile:water:formic acid in the following proportion: leu-enkephalin (2 μM), beta-casomorphin (1 μM), angiotensin II (2 μM), angiotensin III (1 μM),

Correspondence to: Christopher Hendrickson; *e-mail:* hendrick@magnet.fsu.edu

Published online: 20 June 2015

bradykinin (1 μM), Substance P (2 μM), and melittin (1.5 μM). All samples were infused at 500 nL/min and ionized by microelectrospray [5]. Fluoranthene was used as received from Sigma-Aldrich for generation of electron transfer dissociation (ETD) reagent ions.

Magnet

The 21 tesla magnet (Bruker Daltonics, Billerica, MA, USA) room temperature bore diameter is 123 mm, the distance to field center is 1047 mm, and the overall length is 2272 mm. A set of eight cryoshims was used to achieve magnet spatial inhomogeneity less than 5 ppm over a 60 mm diameter by 100 mm long cylinder, which closely matches the working volume of the ICR cell. After shimming the magnet with only the NMR probe inside the magnet bore, the magnet axial inhomogeneity was rechecked with the ICR vacuum chambers and turbopumps in place. The measured difference was less than 1 ppm across the axial length of the ICR cell, so no effort was made to re-shim. No ferroshims were used but could be incorporated in the future, which would reduce the bore diameter to ~104 mm. The measured magnet drift rate was ~4 ppb/h two months after energization and has settled to less than 2 ppb/h after eight months of operation. The magnet cryostat is divided into two thermally separate regions. The lower section contains the complete set of magnet coils and ~1500 L of liquid helium. The upper section stores ~500 L of liquid helium at 4.2 K. A lambda refrigerator uses vaporization and gas expansion of liquid helium from the upper cryostat to cool liquid helium (and the magnet coils) in the lower cryostat to ~2.17 K, which allows magnet operation at 21 tesla. The magnet features a closed cryogenic system with no liquid nitrogen and negligible loss of liquid helium. Instead, the magnet is cooled by a pair of two-stage cryocoolers. The first stages are used to cool shields within the cryostat to ~50 K and the second stages cool surfaces in the upper cryostat to ~4 K to liquefy the helium gas generated by the lambda refrigerator and any boil-off from the upper bath. The cryocoolers and lambda refrigerator vacuum pump operate on an annual maintenance interval, at which time liquid helium can be added if necessary.

FT-ICR Mass Spectrometer

A schematic of the instrument is shown in Figure 1. The mass spectrometer combines a modified Velos Pro [6–8] (ThermoFisher Scientific, San Jose, CA, USA) with an NHMFL-designed external linear quadrupole ion trap, quadrupole ion transfer optics, and novel dynamically harmonized ICR ion trap (DHC) [9, 10]. The Velos Pro front end offers high sensitivity, efficient ion isolation, precise control of ion number, and both collisional dissociation and front-end electron transfer dissociation (FETD; we use the simpler term "ETD" here).

The instrument was laser-aligned with the magnet bore by use of a set of transparent laser detectors (On-Trak Photonics,

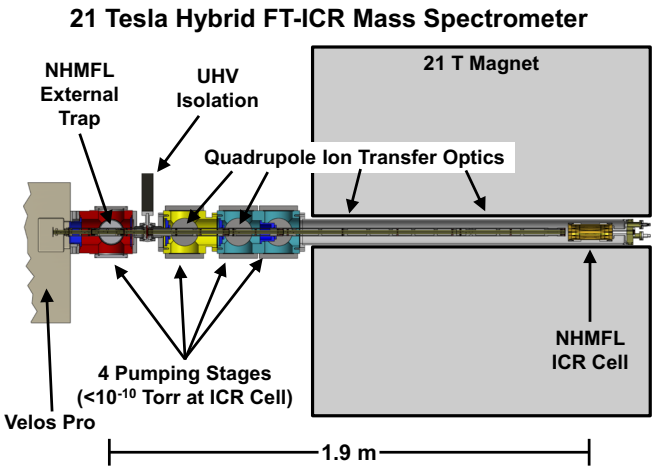


Figure 1. Schematic of the 21 tesla FT-ICR mass spectrometer. Approximately half of the magnet cross-section is shown. Differentially pumped vacuum chambers are shown in red, yellow, and blue (the blue chamber contains two differentially pumped regions, the second of which includes the ICR cell). The scale at bottom shows the approximate distance from the external quadrupole trap to the ICR cell

Irvine, CA, USA) that were centered within the magnet bore and the two main vacuum chambers (before the ion optics or ICR cell were mounted). Digital readout of the offset between the detectors and the laser beam allowed initial centering of the beam in the magnet bore, followed by centering of a 10-way stainless steel block (Kurt J. Lesker, Clairton, PA, USA), and then alignment of a titanium vacuum chamber (Sharon Vacuum, Brockton, MA, USA) onto the block. The residual offset between the beam and the centers of the block and vacuum chamber was less than 25 μm. The vacuum chambers were mounted on extruded aluminum carts (Kanya, Rüti, Switzerland) that translate along steel rails (Thomson, Radford, VA, USA). The rails were aligned with the axis of the magnet such that the maximum offset between the laser beam and the detectors was 1.2 mm as the carts (with mounted chambers) were translated from their final position near the magnet to a distance ~4 m away (along the entire length of the rails). Precise alignment of the mass spectrometer with the magnet is critical for efficient ion injection, and is more critical at higher magnetic field strength because of stronger magnetic mirror force [11].

A set of four differentially turbopumped vacuum chambers reduces pressure from ~10^{-6} Torr (measured in the pumping stage outside the quadrupole accumulator; pressure inside the accumulator is estimated at ~2 mTorr) to less than 10^{-10} Torr at the ICR cell (measured with a residual gas analyzer (Extorr, New Kensington, PA, USA) prior to vacuum chamber insertion into the magnet). The three turbopumps closest to the magnet are magnetically shielded (EXT556HF; Edwards Vacuum, Tewksbury, MA, USA). A force of ~200 Newtons between the magnet and the vacuum cart (which is mostly due to the martensitic pump shields) was measured with a digital scale as the system was rolled into the magnet, under control of a

floor-mounted winch and straps that hold the vacuum cart. A pneumatic gate valve (VAT, Woburn, MA, USA) isolates the three final pumping stages from the rest of the instrument so that UHV pressure is maintained at the ICR cell while the front of the machine is vented for cleaning. A second gate valve (VAT) isolates the first turbopump (Turbo HiPace 700; Pfeiffer Vacuum, Nashua, NH, USA) so that it remains at speed while the front end is vented, which saves ~30 min each vacuum cycle.

A set of two quadrupoles (6.35 mm rod diameter and 5.53 mm device i.d. for each quadrupole, with 62 mm and 86 mm axial length, operated at 2.7 MHz and 300 $V_{p\text{-}p}$) facilitates transfer of ions from the Velos Pro ion trap to the external quadrupole trap [12] (same rod diameter and radial spacing, with 127 mm axial length), which features a set of four interdigitated, angled wires that impose an axial electric field for efficient ion ejection [13]. Auxiliary rf voltage applied to the external quadrupole trap rods (in addition to the ion radial confinement voltage) facilitates *m/z*-independent ion arrival time at the ICR cell [14]. Consequently, ions from *m/z* 200 to 2000 are routinely observed in a single mass spectrum, in spite of long ion flight path (~1.9 m) from the external quadrupole to the ICR cell. External quadrupole trap rf voltage and frequency are typically 1.5 MHz at 250 $V_{p\text{-}p}$, but are broadly adjustable to allow application-specific parameters. Conductance-limiting apertures of 2.5 mm diameter are placed between the 62 and 86 mm quadrupoles, and are used as endcaps for the quadrupole trap. The external quadrupole trap allows more ions to be delivered to the ICR cell by use of multiple fills from the Velos trap (where charge capacity is limited by smaller device size and the need to perform ion isolation [6]). Helium or nitrogen gas is leaked into the quadrupole trap for collisional ion trapping and dissociation. Collisionally-activated dissociation (CAD) is implemented by acceleration of mass-selected ions as they travel from the Velos trap into the external quadrupole trap and collide with nitrogen (or other heavier) gas [15], which provides fragmentation similar to triple quadrupole instruments (which is particularly effective for high sequence coverage of proteins) and activation energy for separation of ETD reduced-charge precursor ions [16]. Multiple fills of the external quadrupole trap were used to build a larger ion population for delivery to the ICR cell.

Ions are guided through the magnetic field gradient by a set of five quadrupoles that span four stages of pumping. All quadrupoles have the same rod and device diameter as the external quadrupole trap, with lengths of 86, 320, 213, 683, and 430 mm, chosen as appropriate for our implementation of differential pumping. Conductance-limiting apertures of 2.5 mm diameter were placed after each quadrupole, except that no aperture was used between the last two quadrupoles. Each injection quadrupole is driven by a tank circuit (Ardara Technologies, Ardara, PA, USA) specifically tuned for the capacitive load of the quadrupole. Frequencies vary from 2.7 to 3.9 MHz and voltage from 0 to 400 $V_{p\text{-}p}$. The last (lowest pressure) pumping stage contains the last two quadrupole segments. The first is 683 mm long and ends at a magnetic field strength of 7 T. The second (430 mm) is typically held at a DC offset equal to the first quadrupole, but no rf is applied in order to avoid ion loss caused by transient cyclotron resonance [17]. No signal loss is observed for ions above the *m/z* threshold for ejection (compared with 0–400 $V_{p\text{-}p}$ applied at 2.9 MHz), in agreement with simulations at 21 T and experiments at 9.4 T.

The DHC is similar in concept to the design of Boldin and Nikolaev [9] but with several modifications. First, the side electrodes are segmented into 12 biconcave and 12 biconvex electrodes (instead of eight), which allows convenient application of excitation and detection onto 120° cell segments for improved excitation electric field, detection sensitivity, and minimization of third harmonic signals [18]. Excitation and detection on the same 120° segments is accomplished with a novel electronic circuit [19]. Second, the trap endcaps are segmented similarly to the "Infinity" cell [20] (but with only four segments) and rf excitation voltage is capacitively coupled onto the endcap segments, which minimizes axial excitation attributable to excitation electric field inhomogeneity [21]. Finally, extensive SIMION modeling was used to optimize the gaps between biconcave and biconvex electrodes at ~1 mm, which we find to be the best compromise between trapping electric field quality and detection capacitance. All segments of the DHC are gold plated to minimize the impact of patch potentials [22]. A detailed description of cell optimization and advantages will be reported separately.

The ETD hardware is adapted from the Thermo Fusion [23] and follows from the work of Earley et al. [24] Fluoranthene reagent ions are generated by Townsend discharge in an excess of nitrogen gas, in an ionization volume located between the s-lens and the first quadrupole ion guide in the Velos Pro (termed "front-ETD" or "FETD" by the inventors). The analyte and reagent targets are 200,000 charges with a reaction period of 10 ms for dissociation of the 34+ charge state of carbonic anhydrase in the Velos Pro linear trap. Multiple fills (e.g., 20) of the external quadrupole trap were used to build a larger ion population for delivery to the ICR cell. Future work will focus on minimizing the reaction period and a complete description of the hardware and method will be reported separately.

Data Acquisition and Analysis

Trap potentials are 4 V during detection. Ions are excited by linear frequency sweep, typically from 1.85 MHz to 107 kHz at 87 Hz/μs but adjustable depending on desired *m/z* range and ion radius. Detection period ranged from 0.38 to 12 s with sampling rate of 2.73 million samples/s (for BSA and peptide mix) or 5.47 million samples/s (for carbonic anhydrase MS/MS). All data are stored as .raw files and can be processed with Xcalibur (ThermoFisher Scientific, San Jose, CA, USA). Time-domain data can optionally be stored as .dat files and processed with Predator analysis software [25], which is required for absorption mode analysis. All time-domain data are Hanning apodized (except for BSA, for which no apodization was done), zero-filled once, and fast Fourier transformed, either in absorption-mode [26] or magnitude-mode as noted. Frequency-to-*m/z* conversion was performed with a two-term calibration equation [27] (for which the terms depend on the total charge delivered to the external quadrupole accumulator).

Tandem mass spectra are deconvolved by THRASH [28], and ProSight Lite v1.1 is used for fragment ion identification [29].

Results and Discussion

Ultrahigh Resolution

At 21 tesla, ions of *m/z* 200–2000 oscillate at 1.6 MHz–160 kHz, enabling high mass resolving power at high spectral acquisition rate. For example, with absorption-mode processing [26] the isotopic distribution of the 48+ charge state of bovine serum albumin (BSA, 66 kDa) is resolved by use of a 0.38 s detection period (Figure 2), which facilitates top-down proteomic analysis of up to 100 kDa proteins by online LC/MS. Further, Figure 2 exhibits excellent signal-to-noise ratio for a single spectral acquisition (>150:1 for the highest magnitude isotopic peak), which facilitates rapid on-line chromatographic analysis. Longer detection period generates higher resolving power, with resolving power >1 million routinely achievable for BSA and other large proteins. Shown in Figure 3 is an ultrahigh resolution spectrum (12 s detection period) for the isolated 48+ charge state of BSA with greater than 2 million resolving power for the highest magnitude peaks (and slightly lower for other isotopes). To the best of our knowledge, this result represents the highest resolving power ever reported for BSA, and promises high performance analysis of even larger proteins [30, 31]. We processed Figure 3 in magnitude mode and without apodization for direct comparison with prior work [10]. Note that the data shown in Figure 3 is the result of a single acquisition, whereas the prior record was the result of 100 averaged scans. High signal magnitude is evident at the end of the detection period, so that future improvement in the memory depth of the digitizer or implementation of heterodyne

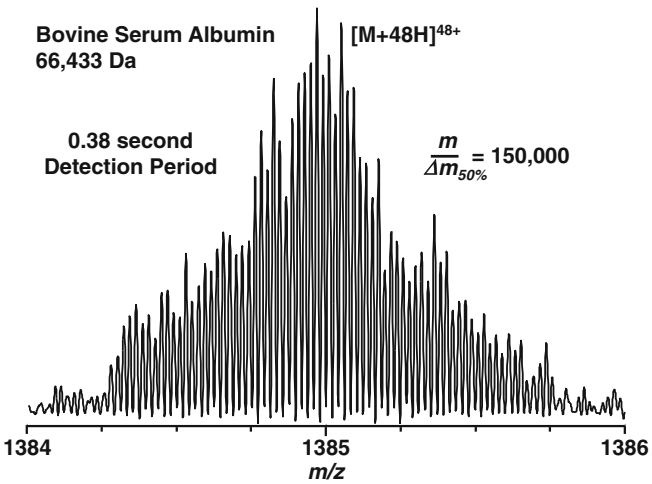


Figure 2. Single-scan electrospray FT-ICR mass spectrum of the isolated 48+ charge state of bovine serum albumin following a 0.38 s detection period. Mass resolving power is approximately 150,000, and the signal-to-noise ratio of the most abundant peak is greater than 150:1. The ion accumulation period was 250 ms and the ion target was 5,000,000

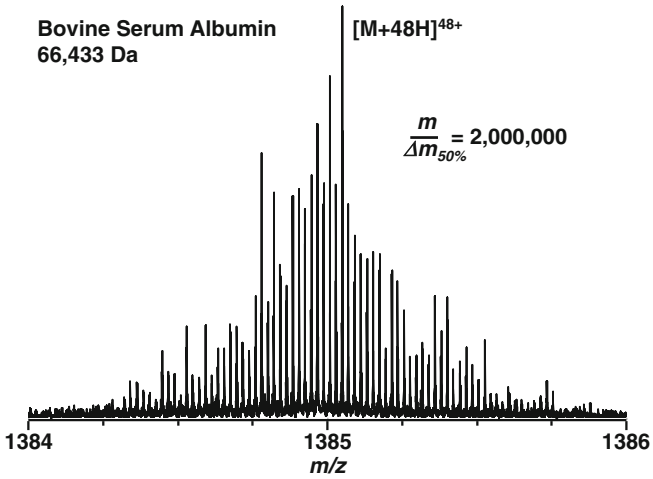


Figure 3. Single-scan electrospray FT-ICR mass spectrum of the isolated 48+ charge state of bovine serum albumin following a 12 s detection period. Mass resolving power is approximately 2,000,000, and the signal-to-noise ratio of the most abundant peak is greater than 500:1. The ion accumulation period was 250 ms and the ion target was 5,000,000

detection should extend the resolving power even further. However, signal for higher charge states (e.g., <*m/z* 1300) damps at much higher rate (resolving power limited to ~500,000), presumably because of nonlinear increase in collision rate caused by higher ion collision cross-section and velocity [32]. Resolving power for higher charge states is, therefore, pressure-limited and lower base pressure is required for higher resolving power of higher charge states.

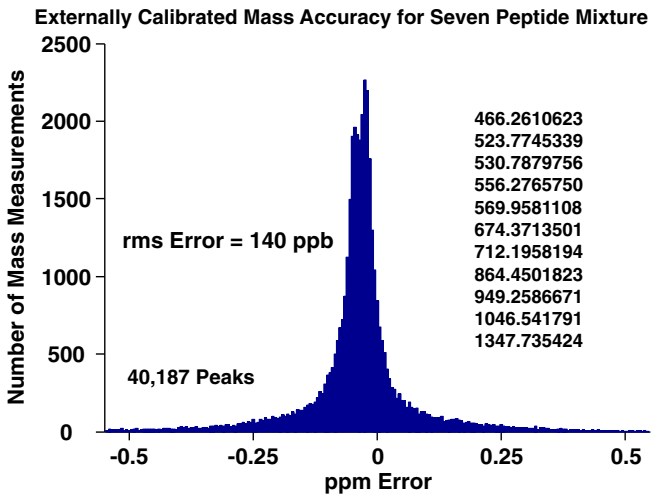


Figure 4. Measured mass error distribution for eleven monoisotopic peaks of seven peptides (multiple charge states are observed for angiotensin II, melittin, and Substance P). Data were collected continuously (3691 spectra) over the course of ~1 h, for which 40,187 total peaks were measured. Mass errors were grouped into 5 ppb bins and plotted as the total number of mass measurements per bin. No signal averaging was used to calculate the error for each measured peak, the ion target was 500,000 for each spectrum, and the ion accumulation period varied from 1.5 to 3 ms

Measured Mass Accuracy

High magnetic field limits the magnitude of ion cyclotron frequency shifts that occur due to ion–ion and ion–image charge forces, and the trapping electric field. Consequently, mass errors due to variation in trapped ion number scale inversely with the square of magnetic field strength [3, 4]. Figure 4 shows typical broadband external calibration mass accuracy for direct infusion of a seven peptide mixture (measured *m/z* varies from 466 to 1347) at 0.76 s detection period, resulting in 300,000 resolving power (magnitude-mode) at *m/z* 400. Variation in measured masses is limited to 140 ppb rms over thousands of measurements (taken over the course of ~1 h). Residual error increases with *m/z*, as expected because of lower mass resolving power but could also be caused by ion cyclotron radius distribution [33] and/or *m/z*-dependent ion cloud focusing in the quadrupole ion optics. For example, exclusion of the Substance P peak at *m/z* 1347 and the angiotensin II peak at *m/z* 1046 reduces the overall rms error to 85 ppb. Alternatively, extension of the detection period to 1.5 s (i.e., 600,000 resolving power at *m/z* 400) improves the measured mass accuracy to 86 ppb rms, and single ion monitoring reduces the error to <50 ppb (data not shown). Future work will focus on isolation and quantitation of *m/z*-dependent systematic mass errors.

MS/MS

Efficient dissociation methods and high magnetic field facilitate rapid acquisition of high resolution tandem mass spectra of large proteins. For example, electron transfer and collisional dissociation combine (in separate experiments) to produce hundreds of fragment ions of carbonic anhydrase, resulting in 68% overall sequence coverage (i.e., we observe at least one cleavage product from 142 of the 258 peptide bonds in carbonic anhydrase), as illustrated in Figure 5. As shown in Figures 6 and 7, overlapping isotopic multiplets are easily resolved (mass resolving power is greater than 150,000 at *m/z* 800), even at high (0.76 s detection period) spectral acquisition rate. Analysis of the electron transfer dissociation spectrum results in 421 detected isotopic multiplets (4553 individual peaks), for which

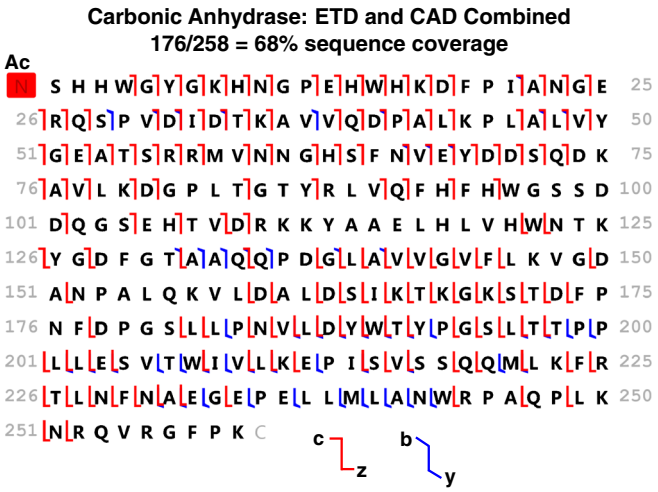


Figure 5. Total sequence coverage for carbonic anhydrase, based on the combined results from electron transfer dissociation of the 34+ charge state and collisional dissociation of the 36+ charge state

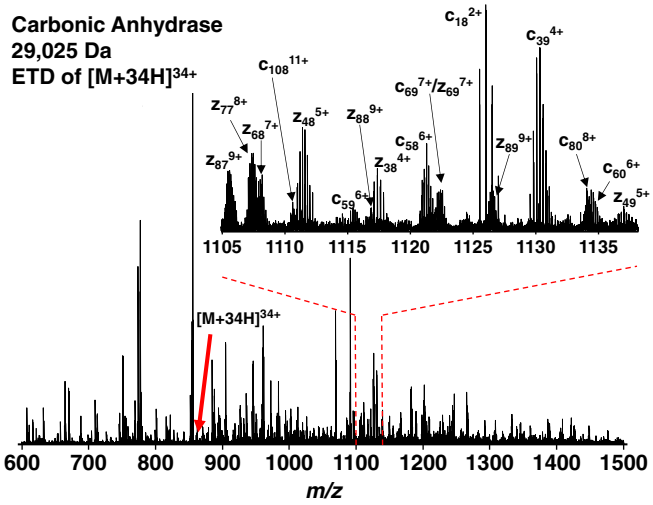


Figure 6. Electron transfer dissociation FT-ICR mass spectrum (100 acquisition average) of the 34+ charge state of carbonic anhydrase. Mass resolving power is greater than 150,000 at *m/z* 800 for a 0.76 s detection period. Identification of 223 isotopic multiplets results in 58% sequence coverage. The ion and reagent target values were 4,000,000 (20 external quadrupole trap fills at 200,000 charges/fill, 0.5 s total accumulation period)

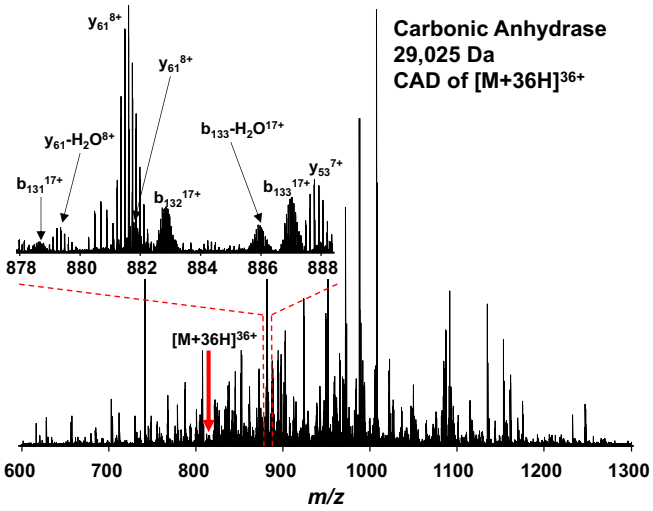


Figure 7. Collisional dissociation FT-ICR mass spectrum (100 acquisition average) of the 36+ charge state of carbonic anhydrase. Mass resolving power is greater than 150,000 at *m/z* 800 for a 0.76 s detection period. Identification of 66 isotopic multiplets results in 21% sequence coverage. The ion target value was 600,000 (three external quadrupole trap fills at 200,000 charges/fill, 0.09 s total accumulation period)

53% are assigned to c or z ions and 58% sequence coverage is observed (Figure 6). Analysis of the collisional dissociation spectrum results in 313 detected multiplets (3753 individual peaks), for which 21% are assigned as b or y ions and 21% sequence coverage is observed (Figure 7). Future work will focus on increasing the speed and efficiency of fragmentation and identification of additional fragments (e.g., internal fragments and/or neutral losses other than water). A barium fluoride window on the ICR cell flange enables future implementation of photodissociation induced by UV (193 [34] or 266 nm), vis (532 nm), or IR (10.6 micron) photons.

Conclusion

The first 21 tesla FT-ICR mass spectrometer is installed at the National High Magnetic Field Laboratory in Tallahassee, Florida. The instrument features a unique combination of resolving power, speed, mass accuracy, and dynamic range (e.g., 300,000 resolving power at *m/z* 400 and 1 Hz spectral acquisition rate, with <150 ppb rms mass accuracy and 1000:1 dynamic range). Unit mass resolving power is achieved at 2 Hz spectral acquisition rate for proteins as large as bovine serum albumin (66 kDa), and 2,000,000 resolving power is demonstrated for a 12 s detection period. Collisional and electron transfer dissociation offer efficient protein structural characterization, and UV photodissociation [34] is planned. We expect the first applications of the instrument to focus on top-down proteomics [35], mapping contact surfaces in large protein complexes by hydrogen–deuterium exchange [36], and petroleomics [37]. The instrument is part of the NSF High Field FT-ICR Mass Spectrometry User Facility, so research directions will ultimately be chosen by user interest. More information can be found at https://nationalmaglab.org/user-facilities/icr.

Acknowledgments

This work was supported by NSF Division of Chemistry (CHE-1016942 and CHE-1019193), NSF Division of Materials Research (DMR-11-57490), and the State of Florida. Many people contributed substantially to specification, acquisition, and installation of the magnet, including Matt Barrios, Greg Boebinger, Kenny Braverman, Richard Brooks, Alfie Brown, Robert Carrier, Tray Cone, Sean Coyne, Brian Fairhurst, Dan Freeman, Jean Futrell, Kevin Gamble, Neil Kelleher, John Kynoch, Denis Markiewicz, Lynn Mayfield, Chris Oxendine, Tom Painter, Marshall Wood, and Aaron Young. The authors thank Dan McIntosh and Vaughan Williams for fabrication of custom mass spectrometer parts, and John Syka, Don Hunt, and ThermoFisher Scientific for help with the ETD hardware and software.

The authors declare no competing financial interest.

References

1. Marshall, A.G., Hendrickson, C.L., Jackson, G.S.: Fourier transform ion cyclotron resonance mass spectrometry: a primer. Mass Spectrom. Rev. **17**, 1–35 (1998)
2. Xian, F., Hendrickson, C.L., Marshall, A.G.: High resolution mass spectrometry. Anal. Chem. **84**, 708–719 (2012)
3. Marshall, A.G., Guan, S.: Advantages of high magnetic field for Fourier transform ion cyclotron resonance mass spectrometry. Rapid Commun. Mass Spectrom. **10**, 1819–1823 (1996)
4. Schaub, T.M., Hendrickson, C.L., Horning, S., Quinn, J.P., Senko, M.W., Marshall, A.G.: High-performance mass spectrometry: Fourier transform ion cyclotron resonance at 14.5 Tesla. Anal. Chem. **80**, 3985–3990 (2008)
5. Emmett, M.R., Caprioli, R.M.: Micro-electrospray mass spectrometry: ultra-high-sensitivity analysis of peptides and proteins. J. Am. Soc. Mass Spectrom. **5**, 605–613 (1994)
6. Schwartz, J.C., Senko, M.W., Syka, J.E.P.: A two-dimensional quadrupole ion trap mass spectrometer. J. Am. Soc. Mass Spectrom. **13**, 659–669 (2002)
7. Second, T.P., Blethrow, J.D., Schwartz, J.C., Merrihew, G.E., MacCoss, M.J., Swaney, D.L., Russell, J.D., Coon, J.J., Zabrouskov, V.: Dual-pressure linear ion trap mass spectrometer improving the analysis of complex protein mixtures. Anal. Chem. **81**, 7757–7765 (2009)
8. Weisbrod, C.R., Hoopmann, M.R., Senko, M.W., Bruce, J.E.: Performance evaluation of a dual linear ion trap-Fourier transform ion cyclotron resonance mass spectrometer for proteomics research. J. Proteome **88**, 109–119 (2013)
9. Boldin, I.A., Nikolaev, E.N.: Fourier transform ion cyclotron resonance cell with dynamic harmonization of the electric field in the whole volume by shaping of the excitation and detection electrode assembly. Rapid Commun. Mass Spectrom. **25**, 122–126 (2011)
10. Nikolaev, E.N., Boldin, I.A., Jertz, R., Baykut, G.: Initial experimental characterization of a new ultra-high resolution FTICR cell with dynamic harmonization. J. Am. Soc. Mass Spectrom. **22**, 1125–1133 (2011)
11. Chen, F.F.: Introduction to Plasma Physics and Controlled Fusion, 2nd edn., pp. 30-34, Plenum Press, New York (1984)
12. Senko, M.W., Hendrickson, C.L., Emmett, M.R., Shi, S.D.H., Marshall, A.G.: External accumulation of ions for enhanced electrospray ionization Fourier transform ion cyclotron resonance mass spectrometry. J. Am. Soc. Mass Spectrom. **8**, 970–976 (1997)
13. Wilcox, B.E., Hendrickson, C.L., Marshall, A.G.: Improved ion extraction from a linear octopole ion trap: SIMION analysis and experimental demonstration. J. Am. Soc. Mass Spectrom. **13**, 1304–1312 (2002)
14. Kaiser, N.K., Savory, J.J., Hendrickson, C.L.: Controlled ion ejection from an external trap for extended m/z range in FT-ICR mass spectrometry. J. Am. Soc. Mass Spectrom. **25**, 943–949 (2014)
15. Patrie, S.M., Charlebois, J.P., Whipple, D., Kelleher, N.L., Hendrickson, C.L., Quinn, J.P., Marshall, A.G., Mukhopadhyay, B.: Construction of a hybrid quadrupole/Fourier transform ion cyclotron resonance mass spectrometer for versatile MS/MS above 10 kDa. J. Am. Soc. Mass Spectrom. **15**, 1099–1108 (2004)
16. Horn, D.M., Ge, Y., McLafferty, F.W.: Activated ion electron capture dissociation for mass spectral sequencing of larger (42 kDa) proteins. Anal. Chem. **72**, 4778–4784 (2000)
17. Beu, S.C., Hendrickson, C.L., Marshall, A.G.: Excitation of radial ion motion in an rf-only multipole ion guide immersed in a strong magnetic field gradient. J. Am. Soc. Mass Spectrom. **22**, 591–601 (2011)
18. Hendrickson, C.L., Beu, S.C., Blakney, G.T., Kaiser, N.K., McIntosh, D.G., Quinn, J.P., Marshall, A.G.: Optimized cell geometry for Fourier transform ion cyclotron resonance mass spectrometry. Proceedings of the 57th ASMS Conference on Mass Spectrometry and Allied Topics, May 31-June 4, Philadelphia, PA (2009)
19. Chen, T., Beu, S.C., Kaiser, N.K., Hendrickson, C.L.: Optimized circuit for excitation and detection with one pair of electrodes for improved Fourier transform ion cyclotron resonance mass spectrometry. Rev. Sci. Instrum. **85**, 066107 (2014)
20. Caravatti, P., Allemann, M.: The 'Infinity Cell': a new trapped-ion cell with radiofrequency covered trapping electrodes for Fourier transform ion

cyclotron resonance mass spectrometry. Org. Mass Spectrom. **26**, 514–518 (1991)
21. Chen, T., Kaiser, N.K., Weisbrod, C.R., Beu, S.C., Blakney, G.T., Quinn, J.P., McIntosh, D.G., Williams, V., Hendrickson, C.L., Marshall, A.G.: Simulation, construction and experimental characterization of a modified dynamically harmonized FT-ICR cell. Proceedings of the 62nd ASMS Conference on Mass Spectrometry and Allied Topics, June 15-19, Baltimore, MD (2014)
22. Camp, J.B., Darling, T.W., Brown, R.E.: Macroscopic variations of surface potentials of conductors. J. Appl. Phys. **69**, 7126–7129 (1991)
23. Senko, M.W., Remes, P.M., Canterbury, J.D., Mathur, R., Song, Q., Eliuk, S.M., Mullen, C., Earley, L., Hardman, M., Blethrow, J.D., Bui, H., Specht, A., Lange, O., Denisov, E., Makarov, A., Horning, S., Zabrouskov, V.: Novel parallelized quadrupole/linear ion trap/Orbitrap Tribrid mass spectrometer improving proteome coverage and peptide identification rates. Anal. Chem. **85**, 11710–11714 (2013)
24. Earley, L., Anderson, L.C., Bai, D.L., Mullen, C., Syka, J.E.P., English, A.M., Dunyach, J.J., Stafford, G.C., Shabanowitz, J., Hunt, D.F., Compton, P.D.: Front-end electron transfer dissociation: a new ionization source. Anal. Chem. **85**, 8385–8390 (2013)
25. Blakney, G.T., Hendrickson, C.L., Marshall, A.G.: Predator data station: a fast data acquisition system for advanced FT-ICR MS experiments. Int. J. Mass Spectrom. **306**, 246–252 (2011)
26. Xian, F., Hendrickson, C.L., Blakney, G.T., Beu, S.C., Marshall, A.G.: Automated broadband phase correction of Fourier transform ion cyclotron resonance mass spectra. Anal. Chem. **82**, 8807–8812 (2010)
27. Ledford Jr., E.B., Rempel, D.L., Gross, M.L.: Space charge effects in Fourier transform mass spectrometry. II. Mass calibration. Anal. Chem. **56**, 2744–2748 (1984)
28. Horn, D.M., Zubarev, R.A., McLafferty, F.W.: Automated reduction and interpretation of high resolution electrospray mass spectra of large molecules. J. Am. Soc. Mass Spectrom. **11**, 320–332 (2000)
29. Fellers, R.T., Greer, J.B., Early, B.P., Yu, X., LeDuc, R.D., Kelleher, N.L., Thomas, P.M.: ProSight Lite: graphical software to analyze top-down mass spectrometry data. Proteomics **00**, 1–4 (2015)
30. Kelleher, N.L., Senko, M.W., Siegel, M.M., McLafferty, F.W.: Unit resolution mass spectra of 112 kDa molecules with 3 Da accuracy. J. Am. Soc. Mass Spectrom. **8**, 380–383 (1997)
31. Valeja, S.J., Kaiser, N.K., Xian, F., Hendrickson, C.L., Rouse, J.C., Marshall, A.G.: Unit mass baseline resolution for an intact 148 kDa therapeutic monoclonal antibody by Fourier transform ion cyclotron resonance mass spectrometry. Anal. Chem. **83**, 8391–8395 (2011)
32. Tolmachev, A.V., Robinson, E.W., Pasa-Tolic, L., Smith, R.D.: FT-ICR optimization for the analysis of intact proteins. Int. J. Mass Spectrom. **287**, 32–38 (2009)
33. Kaiser, N.K., McKenna, A.M., Savory, J.J., Hendrickson, C.L., Marshall, A.G.: Tailored ion radius distribution for increased dynamic range in FT-ICR mass analysis of complex mixtures. Anal. Chem. **85**, 265–272 (2013)
34. Shaw, J.J., Li, W., Holden, D.D., Zhang, Y., Griep-Raming, J., Fellers, R.T., Early, B.P., Thomas, P.M., Kelleher, N.K., Brodbelt, J.S.: Complete protein characterization using top-down mass spectrometry and ultraviolet photodissociation. J. Am. Chem. Soc. **135**, 12646–12651 (2013)
35. Dang, X., Scotcher, J., Wu, S., Chu, R.K., Tolic, N., Ntai, I., Thomas, P.M., Fellers, R.T., Early, B.P., Zheng, Y., Durbin, K.R., LeDuc, R.D., Wolff, J.J., Thompson, C.J., Pan, J., Han, J., Shaw, J.J., Salisbury, J.P., Easterling, M., Borchers, C.H., Brodbelt, J.S., Agar, J.N., Pasa-Tolic, L., Kelleher, N.L., Young, N.L.: The first pilot project of the consortium for top-down proteomics: a status report. Proteomics **14**, 1130–1140 (2014)
36. Zhang, Q., Chen, J., Kuwajima, K., Zhang, H.-M., Xian, F., Young, N.L., Marshall, A.G.: Nucleotide-induced conformational changes of tetradecameric GroEL mapped by H/D echange monitored by FT-ICR mass spectrometry. Sci. Rep. **3**, 1247 (2013)
37. Rodgers, R.P., McKenna, A.M.: Petroleum analysis. Anal. Chem. **83**, 4665–4687 (2011)